

Tyrosine Kinase Inhibitors. 19. 6-Alkynamides of 4-Anilinoquinazolines and 4-Anilino-*pyrido*[3,4-*d*]pyrimidines as Irreversible Inhibitors of the erbB Family of Tyrosine Kinase Receptors

Sylvester R. Klutchko,[†] Hairong Zhou,[†] R. Thomas Winters,[†] Tuan P. Tran,[†] Alexander J. Bridges,[†] Irene W. Althaus,[†] Danielle M. Amato,[†] William L. Elliott,[†] Paul A. Ellis,[†] Mary Ann Meade,[†] Billy J. Roberts,[†] David W. Fry,[†] Andrea J. Gonzales,[†] Patricia J. Harvey,[†] James M. Nelson,[†] Veronica Sherwood,[†] Hyo-Kyung Han,[†] Gerry Pace,[†] Jeff B. Smaill,[‡] William A. Denny,[‡] and H. D. Hollis Showalter^{*,†,§}

Pfizer Global Research and Development, Michigan Laboratories, 2800 Plymouth Road, Ann Arbor, Michigan 48106-1047, and Auckland Cancer Society Research Centre, School of Medical Sciences, The University of Auckland, Private Bag 92019, Auckland 1020, New Zealand

Received September 20, 2005

Structure–activity relationships for inhibition of erbB1, erbB2, and erbB4 were determined for a series of alkynamide analogues of quinazoline- and *pyrido*[3,4-*d*]pyrimidine-based compounds. The compounds were prepared by coupling the appropriate 6-aminoquinazolines or 6-aminopyrido[3,4-*d*]pyrimidines with alkynoic acids, using EDCI·HCl in pyridine. The compounds showed pan-erbB enzyme inhibition but were on average about 10-fold more potent against erbB1 than against erbB2 and erbB4. For cellular inhibition, the nature of the alkylating side chains was an important determinant, with 5-dialkylamino-2-pentynamide type Michael acceptors providing the highest potency. This is suggested to be due to an improved ability of the amine to participate in an autocatalysis of the Michael reaction with enzyme cysteine residues. *Pyrido*[3,4-*d*]pyrimidine analogue **39** was selected for in vivo evaluation and achieved tumor regressions at 10 mg/kg in the A431 human epidermoid carcinoma and at 40 mg/kg for the SF767 human glioblastoma and the SKOV3 human ovarian carcinoma. Complete stasis was observed at 40 mg/kg in the BXP3 human pancreatic carcinoma as well as in the H125 human non-small-cell lung carcinoma.

Introduction

A significant proportion of human tumors overexpress growth factor receptor tyrosine kinase enzymes of the erbB family, and this overexpression is associated with poor prognosis of the disease.^{1–3} Inhibitors of growth factor signaling through these pathways, especially via erbB1 (EGFr, HER-1) and erbB2 (HER-2, neu), have thus been sought as potential anticancer drugs.⁴ The most widely studied class of small molecule inhibitors are the 4-anilinoquinazolines⁵ and related 4-anilino-*pyrido*[*d*]pyrimidines.⁶ These have proved to be potent and selective reversible inhibitors of erbB1 receptor tyrosine kinase activity, through competitive binding to the ATP site of the enzyme.⁷ The 4-anilinoquinazolines gefitinib (ZD-1839, Iressa; **1**)^{8,9} and erlotinib (OSI-774, Tarceva; **2**)¹⁰ have both been approved for the treatment of non-small-cell lung cancer (NSCLC). Responses to treatment with gefitinib^{11,12} and erlotinib¹³ have particularly been observed in a subgroup of NSCLC patients that were identified to have somatic mutations in the tyrosine kinase domain of erbB1. It has, however, been reported that the binding affinities of gefitinib and erlotinib to nine clinically relevant NSCLC erbB1 mutants are comparable to those of the wild-type receptor,¹⁴ supporting the possibility that cells containing an activating mutation are intrinsically more sensitive to erbB1 inhibition.¹⁵ A secondary mutation (T790M) in the kinase domain of erbB1 has been reported in three of six cases of acquired resistance to gefitinib and erlotinib treatment.^{16,17} (See Chart 1 for formulas.)

Further development of reversible inhibitors has focused on improving the clinical efficacy of this class of molecules by

increasing their potency against erbB2. This has generally been achieved by incorporating additional lipophilic bulk in the 4-position of the aniline ring, such as in Lapatinib (GW572016; **3**),¹⁸ which is a potent dual inhibitor of erbB1 and erbB2 currently in phase III clinical trials against breast cancer.⁴ Lapatinib is reported to have a slow inhibitor off-rate consistent with its prolonged effect on down-regulating receptor tyrosine phosphorylation in tumor cells. This slow off-rate may in part be explained by the crystal structure of Lapatinib bound to an inactive-like conformation of erbB1.¹⁹ BMS-599626 (**4**) is another example of a reversible inhibitor with dual activity against erbB1 and erbB2 reported to be in phase I clinical trials.^{20,21} AEE788 (**6**), an analogue of the dual erbB1/erbB2 inhibitor PKI-166 (**5**),²² is also in phase I trials and represents the next generation of multitargeted tyrosine kinase inhibitors possessing potent activity against erbB1, erbB2, and the VEGF receptors.²³

Crystal structures of **2** binding to the ATP site of the erbB1 kinase domain²⁴ and of the related 4-anilinoquinazoline (**7**) bound to the related p38 serine-threonine kinase²⁵ show that the quinazoline chromophore binds to a narrow hydrophobic pocket in the N-terminal domain normally occupied by the adenine of ATP. It is stabilized by hydrogen bonds from the enzyme to the quinazoline N1 and N3 atoms (the latter through a bridging water molecule) with positions C-6 and C-7 of the quinazoline pointing toward the mouth of the channel. These observations are broadly supportive of the binding model proposed earlier.⁷ This model, in conjunction with a homology model built by the Wyeth group, has been used in the design of the quinoline-3-carbonitriles (e.g., **8**) by replacing the N3 atom with a cyano group that can displace the bound water molecule.²⁶

Because these compounds are considered to work by a blockade of the binding of ATP, which is at high concentrations in cells, the use of irreversible inhibitors is attractive. The

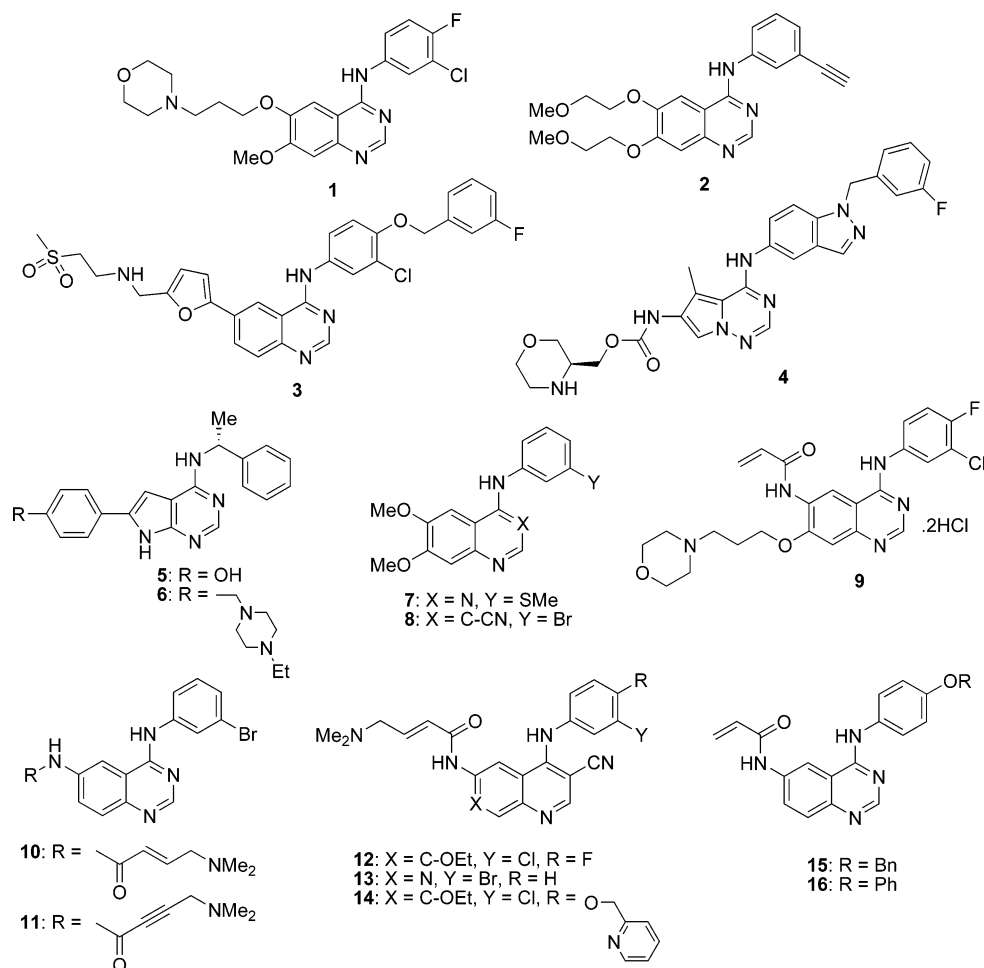
* Corresponding author. Telephone: 734-649-5478. Fax: 734-647-8430. E-mail: showalh@umich.edu.

[†] Pfizer Global Research and Development.

[‡] The University of Auckland.

[§] Current address. College of Pharmacy, University of Michigan, Ann Arbor, MI 48109.

Chart 1. Formulas

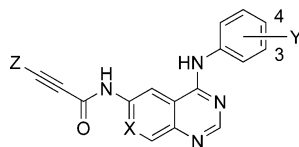


observation that the erbB family of enzymes contains a unique unpaired cysteine residue (Cys 773 in erbB1, Cys 784 in erbB2, and Cys 778 in erbB4) close to the entrance of the ATP binding site, in a position normally occupied by a glutamine or serine in other kinases,²⁷ prompted work on irreversible inhibitors possessing Michael acceptors at the 6-position, positioned to react with this cysteine.²⁸ Development of this concept^{29,30} resulted in the drug canertinib dihydrochloride (CI-1033; **9**), which is currently in phase II clinical trials.^{31,32} In this compound the Michael acceptor of choice is the acrylamide moiety. Other Michael acceptors have also been evaluated, including vinylsulfonamides, vinylsulfones, vinylsulfines,³³ and butynamides.^{34,35} All but the vinylsulfines had some utility for providing irreversible inhibition of erbB1. Despite **9** featuring a similar erbB1 selective reversible binding core to gefitinib, it possesses more potent activity against all members of the erbB family (see Tables 1 and 2). Clearly alkylation of the key cysteine of erbB2 and erbB4 can result in improved potency against these receptors. Potent inhibition of erbB3 (which does not contain a cysteine in this region) by this compound is consistent with erbB3 only being able to acquire signaling potential through heterodimerization with another erbB receptor.⁴

In our initial structure–activity studies around the Michael acceptor we probed the acrylamide nitrogen, the α -carbon, and the β -carbon with a methyl substituent³³ and found that only the acrylamide nitrogen would tolerate an alkyl substituent while still providing fully irreversible inhibition of erbB1. Further elaboration to introduce a soluble side chain at this position was not tolerated. The Wyeth group has independently shown

that amines pendent off the α - and β -carbons of the Michael acceptor through a methylene spacer are well-tolerated and can in some instances provide potent irreversible inhibition of erbB1.³⁴ The dimethylamino crotonamide Michael acceptor of compound **10** is the most widely studied, with the dimethylamino moiety proposed to serve as an intramolecular base catalyst between the Cys 773 sulfhydryl group and the Michael acceptor through a cyclic five-membered ring mechanism.^{34,36} Compound **10** and its dimethylamino butynamide analogue (**11**) showed potent inhibition of erbB1 (isolated enzyme IC₅₀'s 0.011 and 0.006 μ M, respectively) and erbB2 (isolated enzyme IC₅₀'s 0.301 and 0.014 μ M, respectively).

Applying the dimethylamino crotonamide Michael acceptor to the quinoline-3-carbonitrile class of compounds has led to EKB-569 (**12**)³⁶ which is in clinical trial.³⁷ Interestingly this compound is a potent irreversible inhibitor of erbB1 (isolated enzyme IC₅₀ = 0.08 μ M) but is less effective against erbB2 (isolated enzyme IC₅₀ = 1.23 μ M) suggesting that this Michael acceptor will provide erbB2 potency on a quinazoline core (such as for **10**) but not on an analogous quinoline-3-carbonitrile core. Application of this Michael acceptor to the 1,7-naphthyridine core as in compound **13** also provides potent and presumably irreversible inhibition of erbB1; however no erbB2 data have been reported.³⁸ We have previously reported in the 6-acrylamidoquinazoline series that introduction of a benzyloxy or phenoxy substituent at the 4-position of the aniline ring, such as in compounds **15** and **16**, is well-tolerated and can provide irreversible inhibitors with cellular potency against erbB1 and erbB2.²⁹ Optimization of the quinoline-3-carbonitriles to improve their erbB2 potency has proceeded along similar lines

Table 1. Kinase Inhibitory Properties of 6-Substituted 4-Anilinoquinazolines and 4-Anilino-3,4-dihydropyridopyrimidines Bearing Alkynamide Michael Acceptors

compd.	X	Y	Z	IC ₅₀ (nM) ^a				
				erbB1	erbB2	erbB4	autophos (EGF) ^b	autophos (HER) ^c
9				3.0	20	31	1.7	7.4
19^d	CH	3-Br	H	1.6	1.9	1.7	2.7	
20^e	CH	3-Br	Me	0.2	17	12	2.5	
21	CH	3-Cl, 4-F	CH ₂ OH	1.4	2.1	7.3	25	43
22	CH	3-Cl, 4-F	CH ₂ N(Et) ₂	3.1	46	310	6.8	7.5
23	CH	3-Cl, 4-F	CH ₂ N(<i>i</i> -Pr) ₂	4.2	2.8	11	11	65
24	CH	3-Cl, 4-F	CH ₂ N(<i>n</i> -Bu) ₂	40	464	624	11	32
25	CH	3-Cl, 4-F	CH ₂ Nmorpholide	86	300	229	31	173
26	CH	3-Cl, 4-F	(CH ₂) ₂ N(Et) ₂	1.8	2.6	16	4.5	23
27	CH	3-Cl, 4-F	(CH ₂) ₂ Nmorpholide	1.7	2.3	4.3	12	7.6
28^d	N	3-Br	H	0.6	2.4	13	15	
29	N	3-Cl, 4-F	Me	0.3	1.1	0.5	2.5	24
30	N	3-Cl, 4-F	<i>n</i> -Pr	1.7	3.8	2.4	9.6	170
31	N	3-Cl, 4-F	<i>n</i> -Bu	15	5.4	7.1	4.5	20
32	N	3-Cl, 4-F	CH ₂ N(Et) ₂	15	597	644	48	116
33	N	3-Cl, 4-F	CH ₂ N(<i>i</i> -Pr) ₂	44	>10 ³	538	73	36
34	N	3-Cl, 4-F	CH ₂ N(<i>n</i> -Bu) ₂	17	67	73	49	320
35	N	3-Cl, 4-F	CH ₂ Nmorpholide	3.1	26	6.2	14	22
36	N	3-Cl, 4-F	(CH ₂) ₂ Nmorpholide	1.3	0.8	1.0	1.8	5
37	N	3-Br, 4-F	(CH ₂) ₂ Nmorpholide	1.5	0.7	1.0	4.5	0.5
38	N	3-Cl, 4-F	(CH ₂) ₂ Npiperidine	0.9	2.1	1.8	4.3	2
39	N	3-Cl, 4-F	(CH ₂) ₂ N(4-Me-pz) ^f	0.5	0.7	1.2	1.9	1
40	N	3-Br, 4-F	(CH ₂) ₂ N(4-Me-pz) ^f	1.1	0.5	0.8	2.7	3.5

^a Concentration for 50% inhibition of phosphorylation of a Glu/Tyr copolymer (see Experimental Section). Values are the average of at least two separate determinations, with a CV of $\pm 22\%$. ^b Inhibition of erbB1 autophosphorylation in NIH3T3 cells transfected with the full-length human erbB1 (see Experimental Section). ^c Inhibition of heregulin-stimulated erbB autophosphorylation in MDA-MB-453 human breast carcinoma cells (see Experimental Section). ^d Reference 55. ^e References 34 and 55. ^f 4-Methylpiperazine.

by introducing a 2-pyridinylmethoxy group in the 4-position of the aniline ring resulting in HKI-272 (**14**), a potent irreversible inhibitor of both erbB1 and erbB2, which is reported to be in clinical trial.³⁹ HKI-272 and analogues have been shown to be effective in vitro against NSCLC cells that have acquired resistance to gefitinib, encouragingly including those that have the T790M mutation.⁴⁰

Irreversible inhibitors of the erbB family of tyrosine kinases continue to be of considerable interest clinically. In certain instances the Michael acceptor can confer pan-erbB activity to an otherwise erbB1 selective core structure. In this paper we report on structure–activity relationships for alkynamide analogues of both the quinazolinone and pyrido[3,4-*d*]pyrimidine core structures. We identify a novel Michael acceptor that provides potent pan-erbB activity, and we report data for this against the erbB1, erbB2, and erbB4 kinases.

Chemistry

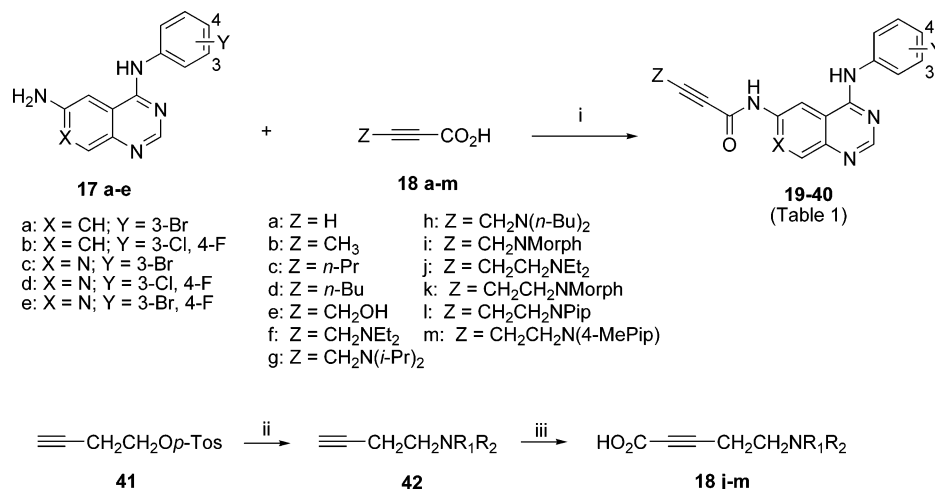
The compounds reported in this paper were made by the generalized routes outlined in Scheme 1. 6-Aminoquinazolines (**17a**⁴¹ and **17b**²⁹) and the corresponding pyrido[3,4-*d*]pyrimidines (**17c**,⁴² **17d**, **17e**²⁹) were coupled with a wide range of alkynoic acids (**18a–m**) to provide target compounds **19–40** (Table 1). In general, the 6-amino moiety of heterocycles **17a–e** was found to be weakly reactive toward the range of activated acids utilized, and this was reflected in the poor yields of purified products (5–32% for quinazolines; 2–28% for pyrido[3,4-*d*]pyrimidines). The most generalized conditions for this amidation were found to be the use of 1-(3-dimethylaminopropyl)-3-ethylcarbodiimide hydrochloride (EDCI·HCl) in pyridine at room temperature. Optimization of coupling conditions was not extensively explored.

The propargylic acids **18a–i** were either commercially available or synthesized by the Wyeth procedure.³⁴ The homologous pentynoic acids **18j–m** were synthesized by modification of a procedure described many years ago,⁴³ with details shown in Scheme 1. Thus, condensation of commercially available 4-(tosyloxy)-1-butyne (**41**) with a range of secondary amines provided 4-(substituted amino)-1-butyne (**42**) in non-optimized yields (31–82%). Subsequent lithiation of **42** with *n*-butyllithium in THF or ether and carboxylation provided target pentynoic acids **18j–m** in 59–77% yield. These either were coupled to **17a–e** as their isolated lithium salts or were converted to their neutral form by passage over an ion-exchange resin. When the lithium salt was utilized, an equivalent of pyridinium hydrochloride was added to buffer the reaction medium.

Results and Discussion

Table 1 lists the structures and kinase inhibitory properties of a series of 6-alkynamide derivatives of both 4-anilinoquinazolines and 4-anilino-3,4-dihydropyridopyrimidines. As in our previous studies,³³ the anilino ring substituent was kept constant (generally 3-chloro-4-fluoro; the substitution pattern used in both gefitinib and canertinib dihydrochloride) to facilitate intercomparisons of the different Michael acceptors. The known compounds **9** (canertinib dihydrochloride), **19**, **20**, and **28** were also included for wider comparison.

All of the compounds in Table 1 were investigated for inhibition of erbB1, erbB2, and erbB4, using cytoplasmic fusion proteins made by cloning the erbB1 sequence (Met-668 to Ala-1211), erbB2 (Ile-675 to Val-1256), and erbB4 sequence (Gly-259 to Gly-690) into baculovirus. The IC₅₀ values shown were determined by an enzyme-linked immunosorbent assay based

Scheme 1^a

^a (i) 1-Ethyl-3-(3'-dimethylaminopropyl)carbodiimide hydrochloride (EDCI·HCl), pyridine, or DMF, 0–25 °C; (ii) HNR₁R₂, DMF, or CH₃CN or THF, 25–85 °C; (iii) *n*-BuLi, THF, –78 °C, then CO₂, ether, –78 to 25 °C.

(ELISA-based) receptor tyrosine kinase assay, with poly(Glu-Tyr) as substrate, and are technically apparent IC₅₀ values.²⁹ They are an average of at least two separate determinations.

Overall, for the compounds where there was a full set of data there was a good correlation between the degree of inhibition of the different isozymes, suggesting that the general class of 6-alkynamides is composed of pan-erbB inhibitors (eqs 1–3; data for eq 2 from compounds **19–40** of Table 1; data for eqs 1 and 3 omit compound **33**). These equations also show that the compounds were on average about 10-fold more potent against erbB1 than against erbB2 and erbB4 (coefficient of IC₅₀ term in eqs 1 and 2).

$$\log \text{IC}_{50}(\text{erbB1}) = 0.54(\pm 0.11) \log \text{IC}_{50}(\text{erbB2}) - 0.05(\pm 0.13) \quad (1)$$

$$n = 21, \quad r = 0.76, \quad s = 0.46, \quad F_{2,19} = 25$$

$$\log \text{IC}_{50}(\text{erbB1}) = 0.54(\pm 0.11) \log \text{IC}_{50}(\text{erbB4}) - 0.11(\pm 0.15) \quad (2)$$

$$n = 22, \quad r = 0.76, \quad s = 0.48, \quad F_{2,20} = 28$$

$$\log \text{IC}_{50}(\text{erbB2}) = 0.91(\pm 0.08) \log \text{IC}_{50}(\text{erbB4}) - 0.06(\pm 0.11) \quad (3)$$

$$n = 21, \quad r = 0.93, \quad s = 0.37, \quad F_{2,19} = 117$$

Over the whole class, there was a less close correlation between the erbB1/EGF autophosphorylation and erbB2/HER autophosphorylation data (*r* values of 0.61 and 0.64, respectively). However, there was a clear advantage in pan-erbB autophosphorylation potency for compounds bearing the 5-dialkylamino-2-pentynamide class of Michael acceptor (such as **26**, **27**, **36–40**). These derivatives were more potent inhibitors of both the isolated enzymes and of autophosphorylation in cells with average IC₅₀ values of 1.25, 1.4, 3.9, 4.5, and 6.1 nM in erbB1, erbB2, erbB4, and EGF- and HER-stimulated autophosphorylation, respectively, compared with average values of 15, 91, 181, 27, and 94 nM, respectively, for all the other compounds in these assays. The latter average figures did not vary greatly if the non-amine-bearing analogues were excluded, suggesting that the important factor was the ability of the amine to participate in an autocatalytic reaction with the key cysteine of the erbB family via a six-membered-ring mechanism, analogous

Table 2. Comparison of the in Vitro and Cellular Kinase Activities of Compound **39** with Other ErbB Family Inhibitors

activity	IC ₅₀ (nM)			
	39	canertinib	gefitinib	erlotinib
EGF receptor (erbB1) ^a	0.5	3.0	3.1	0.6
ErbB2 receptor ^a	0.7	20	343	511
PDGF receptor	> 50 000	> 50 000		
FGF receptor	> 50 000	> 50 000		
insulin receptor	> 50 000	> 50 000		
EGF receptor autophosphorylation ^b	1.9	1.7	14.4	19.3
ligand-regulated erbB2 autophosphorylation ^c	0.8	16	599	299
HER-regulated tyrosine autophosphorylation ^d	1	5.1		

^a See footnotes to Table 1. ^b In erbB1-transfected NIH3T3 cells. ^c In T24 NIH fibroblasts expressing a chimeric receptor with the extracellular binding domain of erbB1 and the intracellular kinase domain of erbB2. ^d In MDA-MB-453 human breast carcinoma cells.

to that reported previously.³⁴ Compounds **37**, **39**, and **40** have been confirmed as irreversible inhibitors of erbB1 in a modified A431-cellular autophosphorylation assay containing a drug wash-out protocol^{28,29} (data not shown).

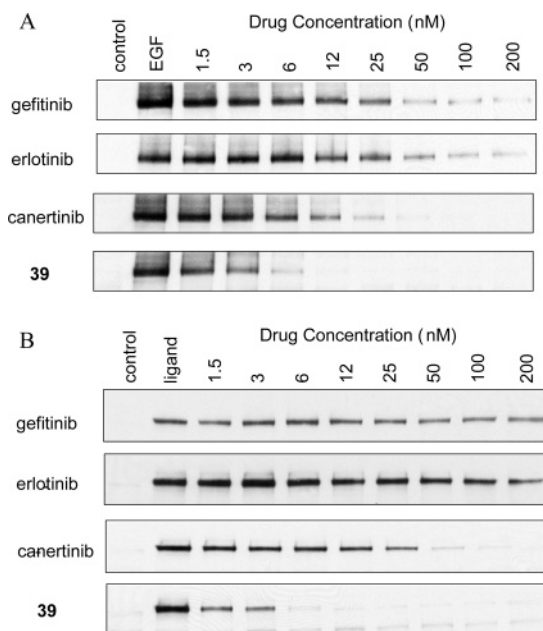
Table 1 also reveals that there is a greater potency in cellular versus enzyme assays for a number of compounds (e.g., **24** and **33**). This is viewed as not being due to mixed erbB inhibition in cells but perhaps to differences in response to different enzyme constructs (i.e., enzyme assays use GST-fusion proteins where GST is fused to the intracellular domain of the erbBs, whereas in the HER-stimulated autophosphorylation cell assay, the wild-type, full length forms are present).

Of the compounds evaluated, the pyrido[3,4-*d*]pyrimidine **39** had the best overall potencies in both the enzymic and cellular assays and was selected for further studies. Table 2 shows that **39** has broadly similar in vitro activity to the clinical irreversible inhibitor canertinib dihydrochloride (**9**) and is significantly more potent (particularly in the erbB2 cellular assay) than the clinically approved reversible inhibitors gefitinib and erlotinib. Furthermore, compound **39** is selective for the erbB family of tyrosine kinases over the PDGF, FGF, and insulin receptor tyrosine kinases. The pan-erbB nature of this compound is assessed in three cellular assays: first, in the EGF-stimulated erbB1 autophosphorylation assay (in erbB1-transfected NIH3T3 cells) (see Figure 1, part A), second, in the ligand-stimulated erbB2 autophosphorylation assay (in T24 NIH fibroblasts

Table 3. In Vivo Antitumor Efficacy of **39** in Mice against a Spectrum of Implanted Human Tumor Xenografts

tumor	dose ^a (mg/kg)	schedule	weight change (%) ^b	T-C ^c	GDI ^d
A431 epidermoid	10	(Q1D × 5) × 2; D15	-1.0	26.9	269
BXPC3 pancreatic	40	(Q1D × 5) × 3; D12	-0.6	16.2	108
H125 NSC lung	40	D17-31	0	17.1	114
SF767 glioblastoma	40	(Q1D × 5) × 3; D15	-0.4	23.8	159
SKOV3 ovarian	40	D17-31	-6.5	21.4	187

^a Dose is PO. ^b Maximum treatment related weight loss, expressed as a percent of initial group weight. ^c T-C is the difference, in days, for the median treated and control tumors to reach a fixed evaluation size, usually 750 mg. ^d GDI (growth delay index) = [(T-C)/treatment days] × 100.

**Figure 1.** A: Inhibition of erbB1 tyrosine kinase activity in NIH 3T3 fibroblasts expressing human erbB1. B: Inhibition of erbB2 tyrosine kinase activity in T24 NIH fibroblasts expressing a chimeric receptor with the extracellular binding domain of erbB1 and the intracellular kinase domain of erbB2.

expressing a chimeric receptor with the extracellular binding domain of erbB1 and the intracellular kinase domain of erbB2) (see Figure 1, part B), and third, in the heregulin-stimulated tyrosine autophosphorylation assay (in erbB2, -3, and -4 expressing MDA-MB-453 cells). Low nanomolar potency across these three assays, as shown for **9** and **39**, is considered indicative of pan-erbB inhibition.

Compound **39** was evaluated for antitumor effects in a variety of implanted human tumor xenografts in immune-deficient mice. These models were chosen due to their expression of erbB receptor family members. A summary of the data is shown (Table 3), depicting the activity obtained at either the maximum tolerated dose (MTD) or the dose where the highest efficacy was obtained. Loss of weight was taken as an indication of

toxicity and in general was very mild. The large decrease in weight for SKOV3 implanted mice appears to be due to effects on the mice by the tumor rather than the drug, since untreated tumor-bearing mice had similar weight losses.

For **39** the inhibition of target receptor activation remained significantly inhibited for at least 24 h in tumors after a single dose over a relatively wide dose range. The most sensitive tumor was the A431 human epidermoid carcinoma, where significant tumor regression was clearly evident (Table 3). Tumor regression in response to **39** was also apparent in the SF767 human glioblastoma and the SKOV3 human ovarian carcinoma. The compound produced complete stasis in the BXPC3 human pancreatic carcinoma as well as in the H125 human non-small-cell lung carcinoma under continuous daily dosing. In general, **39** was highly active in all five tumor models and was as efficacious as canertinib dihydrochloride (**9**) in A431 xenografts.³⁰

Detailed pharmacokinetic studies of **39** were undertaken in rat, monkey, and dog, and the results are summarized in Table 4. In rat and monkey the plasma clearance was higher than hepatic blood flow; this may be related to low metabolic stability in these species (unpublished data) and possibly to irreversible binding of **39** to the target. The total amount of the unchanged parent drug excreted into bile and urine was less than 1% in rats, so that the contribution of biliary and renal clearance to the total plasma clearance was minimal. The volume of distribution was higher than total body water in all species, suggesting that **39** likely distributed to tissue. It exhibited a short plasma half-life (<2 h) in all three species, although the duration of action did not solely rely on this because of its irreversible inhibition mechanism. The bioavailability of **39** (*F*) was 11.4% in rat and 67.8% in dog following a single oral administration of 15 mg/kg under a fasted condition. In monkeys, the bioavailability was 6.75% at a 30 mg/kg dose (Table 4).

Conclusions

The alkyamides in general are potent inhibitors of erbB1, erbB2, and erbB4, being on average the most potent (10×) against erbB1. Analogues bearing a 5-dialkylamino-2-pentynamide class of Michael acceptor are irreversible inhibitors of erbB1 (and presumably erbB2 and erbB4), and possess a potency advantage (6- to 80-fold) in terms of pan-erbB activity in both isolated enzyme and cellular autophosphorylation assays. This is likely due to an improved ability of the amine to participate in autocatalysis of the Michael reaction with cysteine.³⁴ The pyrido[3,4-*d*]pyrimidine **39** had the best overall potencies in both the enzymatic and cellular assays. This compound was evaluated in a panel of five human tumor xenografts in nude mice, by use of a multiple dose schedule. It was highly active in all the models as measured by the growth delay index.

Experimental Section

Analyses were performed by the Analytical Department, Pfizer Global Research and Development, Ann Arbor Laboratories.

Table 4. Mean Pharmacokinetic Parameters of **39** in Rat, Dog, and Monkey, Following a Single Dose Administration

species	dose mg/kg	route	<i>N</i>	<i>C</i> _{max} ng/mL	<i>t</i> _{max} (h)	<i>t</i> _{1/2} (h)	CL (mL/min)/kg	<i>V</i> _{dss} (L/kg)	AUC(0-t _{lqc}) (ng·h/mL)	<i>F</i> (%)
rat	5	iv ^a	3			0.83	118.8	3.1	703	
dog	5	iv ^a	3			1.86	11.5	0.93	7470	
monkey	5	iv ^a	3			0.37	85.8	1.7	1190	
rat	15	po ^b	3	56.3	4.7				240	11.4
dog	15	po ^b	3	4180	1.0				15 200	67.8
monkey	30	po ^b	2	83.5	3.5				485	6.75

^a iv dosing vehicle: 5% DMSO/95% 0.05N methanesulfonic acid in saline (rat); 5% DMA/95% 50 mM lactic acid (pH 4.0) (dog and monkey). ^b po dosing vehicle: 5% PEG/95% methylcellulose (0.5%) (rat); methylcellulose (0.5%) (dog and monkey).

Melting points were determined using a Gallenkamp digital melting point apparatus and are as read. NMR spectra were measured on a Varian Unity 400 MHz spectrometer and referenced to Me₄Si. Mass spectra were recorded on a Finnigan MAT 900Q spectrometer. Column chromatography was carried out with flash silica gel. All reactions were run under an inert atmosphere of nitrogen or argon. All reaction solvents were anhydrous, analytical reagent quality. Solvent drying during extractive workups was carried out with Mg₂-SO₄ unless otherwise noted. 4-(Tosyloxy)-1-butyne (**41**) was purchased from Lancaster Synthesis.

N-[4-[(3-Bromophenyl)amino]-6-quinazoliny]-2-propynamide (19). A stirred solution of 4-[3-bromophenylamino]-6-aminoquinazoline⁴¹ (**17a**) (158 mg, 0.5 mmol) and propiolic acid (**18a**) (0.08 mL, 1.1 mmol) in DMF (1.5 mL) was treated with 1-(3-dimethylaminopropyl)-3-ethylcarbodiimide hydrochloride (EDCI·HCl) (200 mg, 1.04 mmol) under nitrogen at 0 °C. The solution was stirred at 0 °C for 30 min and then quenched with water. The resulting fine precipitate was collected, dissolved in MeOH, and purified by preparative TLC on silica gel. It was eluted with MeOH/CHCl₃ (9:1) to give **19** as a yellow solid (21 mg, 12%); mp > 310 °C. ¹H NMR [(CD₃)₂SO] δ: 11.18 (br s, 1H), 9.94 (s, 1H), 8.75 (s, 1H), 8.59 (s, 1H), 8.15 (s, 1H), 7.85–7.79 (m, 3H), 7.37–7.28 (m, 2H), 4.53 (s, 1H). APCIMS *m/z* (relative intensity): 366 (⁷⁹BrM⁺, 13), 367 (⁷⁹BrMH⁺, 50), 368 (⁸¹BrM⁺, 24), 369 (⁸¹BrMH⁺, 47). Anal. (C₁₇H₁₁N₄BrO) C, H, N.

N-[4-[(3-Bromophenyl)amino]-6-quinazoliny]-2-butynamide (20). A stirred solution of 2-butynoic acid (**18b**) (196 mg, 2.3 mmol) and EDCI·HCl (385 mg, 2.0 mmol) in DMF (5 mL) was treated with 4-[3-bromophenylamino]-6-aminoquinazoline⁴¹ (**17a**) (316 mg, 1.0 mmol) over 20 min at 25 °C. The resulting solution was stirred at 25 °C, and two further lots of EDCI·HCl (206 mg, 1.0 mmol) and 2-butynoic acid (82 mg, 1.0 mmol) were added after 14 and 22 h, respectively. The mixture was stirred at 25 °C for an additional 12 h and then quenched with water. The resulting precipitate was collected and dissolved in MeOH and purified by preparative TLC on silica gel. It was eluted with EtOAc/acetone (1:1) to give **20** as a solid (20 mg, 5%); mp 281–283 °C. ¹H NMR [(CD₃)₂SO] δ: 10.97 (br s, 1H), 9.93 (s, 1H), 8.76 (s, 1H), 8.57 (s, 1H), 8.14 (s, 1H), 7.84–7.76 (m, 3H), 7.34 (t, *J* = 8.1 Hz, 1H), 7.29 (d, *J* = 7.8 Hz, 1H), 2.09 (s, 3H). APCIMS *m/z* (relative intensity): 381 (⁷⁹BrMH⁺, 95), 382 (⁸¹BrM⁺, 23), 383 (⁸¹BrMH⁺, 100). Anal. (C₁₈H₁₃BrN₄O·0.5H₂O) C, H, N.

N-[4-[(3-Chloro-4-fluorophenyl)amino]-6-quinazoliny]-4-(dibutylamino)-2-butynamide (24). A mixture of 6-amino-4-(3-chloro-4-fluoroanilino)quinazoline²⁹ (**17b**) (93 mg, 0.32 mmol), pyridine (0.03 mL, 0.37 mmol), and 4-(dibutylamino)-2-butynoic acid (**18h**) (69 mg, 0.33 mmol) in DMF (1.5 mL) at 0 °C was treated with EDCI·HCl (76 mg, 0.40 mmol). The reaction was slowly warmed to room temperature and quenched with water after 7 h. The mixture was extracted with EtOAc, and the combined organic phases were washed with water and brine, dried, and concentrated to a residue that was purified first by silica gel column chromatography (elution with 2.5% MeOH/CH₂Cl₂) and then by preparative TLC (elution with 10% MeOH/CH₂Cl₂). The purified material was triturated in ether to afford **24** as a light yellow solid (30 mg, 19%); mp 78–79 °C. ¹H NMR [(CD₃)₂SO] δ: 10.9 (s, 1H), 9.89 (s, 1H), 8.66 (s, 1H), 8.52 (s, 1H), 8.07 (dd, *J* = 6.6, 2.5 Hz, 1H), 7.8–7.7 (m, 3H), 7.39 (t, *J* = 9.2 Hz, 1H), 3.55 (s, 2H), 1.4–1.2 (m, 8H), 0.84 (t, *J* = 7.1 Hz, 6H). APCIMS *m/z* (relative intensity): 482 (M⁺, 100). Anal. (C₂₆H₂₉ClFN₅O·0.7H₂O) C, H, N.

4-(Dibutylamino)-2-butynoic acid (18h) was synthesized by the Wyeth procedure.³⁴ ¹H NMR (CD₃OD) δ: 4.18 (s, 2H), 3.23 (m, 4H), 1.69 (m, 4H), 1.43 (dq, *J* = 15.0, 7.4 Hz, 4H), 1.00 (t, *J* = 7.4 Hz, 6H). APCIMS *m/z* (relative intensity): 212 (M⁺, 100), 168 (75).

N-[4-[(3-Chloro-4-fluorophenyl)amino]-6-quinazoliny]-4-hydroxy-2-butynamide (21). A similar reaction of **17b** and 4-hydroxy-2-butynoic acid⁴⁴ (**18e**) provided **21** as a light yellow solid (23%); mp 231–233 °C. ¹H NMR [(CD₃)₂SO] δ: 11.0 (s, 1H), 9.91 (s, 1H), 8.71 (s, 1H), 8.51 (s, 1H), 8.05 (dd, *J* = 6.8, 2.7 Hz, 1H), 7.74–7.70 (m, 3H), 7.39 (t, *J* = 9.3 Hz, 1H), 5.55 (t, *J* = 6.1

Hz, 1H), 4.28 (d, *J* = 5.8 Hz, 2H). APCIMS *m/z* (relative intensity) 371 (M⁺, 100). Anal. (C₁₈H₁₂ClFN₄O₂·0.9H₂O) C, H, N.

N-[4-[(3-Chloro-4-fluorophenyl)amino]-6-quinazoliny]-4-(diethylamino)-2-butynamide (22). A similar reaction of **17b** and 4-(diethylamino)-2-butynoic acid³⁴ (**18f**) provided **22** as a light yellow solid (9%); mp 108–110 °C. ¹H NMR [(CD₃)₂SO] δ: 10.9 (s, 1H), 9.89 (s, 1H), 8.65 (s, 1H), 8.52 (s, 1H), 8.07 (dd, *J* = 6.8, 2.5 Hz, 1H), 7.8–7.73 (m, 3H), 7.39 (t, *J* = 9.2 Hz, 1H), 3.57 (s, 2H), 2.49 (q, *J* = 7.1 Hz, 4H), 0.97 (t, *J* = 7.1 Hz, 6H). APCIMS *m/z* (relative intensity): 426.1 (M⁺, 100). Anal. (C₂₂H₂₁ClFN₅O·0.3C₃H₆O·0.8H₂O) C, H, N.

N-[4-[(3-Chloro-4-fluorophenyl)amino]-6-quinazoliny]-4-(bis(1-methylethyl)amino)-2-butynamide (23). A similar reaction of **17b** and 4-[bis(1-methylethyl)amino]-2-butynoic acid³⁴ (**18g**) provided **23** as a light yellow solid (32%); mp 120–122 °C. ¹H NMR [(CD₃)₂SO] δ: 10.87 (s, 1H), 9.88 (s, 1H), 8.66 (s, 1H), 8.51 (s, 1H), 8.07 (dd, *J* = 6.9, 2.7 Hz, 1H), 7.79–7.72 (m, 3H), 7.39 (t, *J* = 9.3 Hz, 1H), 3.55 (s, 2H), 3.3–3.07 (m, 2H), 1.01 (d, *J* = 6.6 Hz, 12H). APCIMS *m/z* (relative intensity): 454 (M⁺, 100). Anal. (C₂₄H₂₅ClFN₅O·0.5H₂O) C, H, N.

N-[4-[(3-Chloro-4-fluorophenyl)amino]-6-quinazoliny]-4-(4-morpholinyl)-2-butynamide (25). A similar reaction of **17b** and 4-(4-morpholinyl)-2-butynoic acid³⁴ (**18i**) provided **25** as an off-white powder (20%); mp 167–169 °C. ¹H NMR [(CD₃)₂SO] δ: 11.02 (s, 1H), 9.93 (s, 1H), 8.69 (s, 1H), 8.55 (s, 1H), 8.10 (dd, *J* = 6.8, 2.7 Hz, 1H), 7.84–7.77 (m, 3H, H-8), 7.43 (t, *J* = 9.2 Hz, 1H), 3.61 (br, 4H), 3.55 (s, 2H), 2.53 (br, 4H). APCIMS *m/z* (relative intensity): 440 (M⁺, 100). Anal. (C₂₂H₂₁ClFN₅O·0.3C₃H₆O·0.3H₂O) C, H, N.

N-[4-[(3-Chloro-4-fluorophenyl)amino]-6-quinazoliny]-5-(4-diethylamino)-2-pentynamide (26). A similar reaction of **17b** and 5-(diethylamino)-2-pentynoic acid (**18j**) provided **26** as a tan powder (11%); mp 138–140 °C. ¹H NMR [(CD₃)₂SO] δ: 10.87 (s, 1H), 9.89 (s, 1H), 8.68 (s, 1H), 8.51 (s, 1H), 8.05 (dd, *J* = 6.9, 2.7 Hz, 1H), 7.74–7.71 (m, 3H), 7.41 (t, *J* = 9.1 Hz, 1H), 2.69 (t, *J* = 7.2 Hz, 2H), 0.93 (t, *J* = 7.1 Hz, 6H). APCIMS *m/z* (relative intensity): 440 (M⁺, 100). Anal. (C₂₃H₂₃ClFN₅O·0.3H₂O) C, H, N.

N-[4-[(3-Chloro-4-fluorophenyl)amino]-6-quinazoliny]-5-(4-morpholinyl)-2-pentynamide (27). A similar reaction of **17b** and 5-(4-morpholinyl)-2-pentynoic acid (**18k**) provided **27** as a cream powder (11%); mp 155–157 °C. ¹H NMR [(CD₃)₂SO] δ: 10.9 (s, 1H), 9.89 (s, 1H), 8.67 (s, 1H), 8.51 (s, 1H), 8.05 (dd, *J* = 6.9, 2.5 Hz, 1H), 7.4–7.71 (m, 3H), 7.39 (t, *J* = 9.1 Hz, 1H), 3.53 (t, *J* = 4.4 Hz, 4H), 2.58–2.53 (m, 4H), 2.38–2.34 (m, 4H). APCIMS *m/z* (relative intensity): 454 (M⁺, 100). Anal. (C₂₃H₂₁ClFN₅O₂·0.6H₂O) C, H, N.

N-[4-[(3-Bromophenyl)amino]pyrido[3,4-*d*]pyrimidin-6-yl]-2-propynamide (28). A stirred solution of 6-amino-4-[(3-bromophenyl)amino]pyrido[3,4-*d*]pyrimidine⁴² (**17c**) (94 mg, 0.3 mmol) and propiolic acid (**18a**) (66 μL, 1.05 mmol) in pyridine (1.2 mL) under nitrogen at –20 °C was treated with EDCI·HCl (294 mg, 1.5 mmol). After 2.25 h, additional propiolic acid (33 μL) and EDCI·HCl (147 mg) were added, and after a total reaction time of 7.5 h the mixture was diluted with DMF and then poured into EtOAc/water (1:1). The aqueous phase was extracted with EtOAc (2×), and the combined organic phases were washed with brine (2×), dried, and filtered through silica gel. The filtrate was concentrated and purified by column chromatography, then eluted with EtOAc. Product fractions were pooled and concentrated and the residue was triturated in EtOAc/*tert*-butyl methyl ether (1:1) to provide **28** (16 mg, 14%); mp > 150 °C (dec). ¹H NMR [(CD₃)₂SO] δ: 11.69 (s, 1H), 10.31 (s, 1H), 9.05 (s, 1H), 8.83 (s, 1H), 8.68 (s, 1H), 8.15 (s, 1H), 7.87 (d, *J* = 7.2 Hz, 1H), 7.40–7.33 (m, 2H), 4.54 (s, 1H). APCIMS *m/z* (relative intensity): 367 (⁷⁹BrM⁺, 28), 368 (⁷⁹BrMH⁺, 100), 369 (⁸¹BrM⁺, 50), 370 (⁸¹BrMH⁺, 14). Anal. (C₁₆H₁₀BrN₅O·0.2H₂O) C, H, N.

N-[4-[(3-Chloro-4-fluorophenyl)amino]pyrido[3,4-*d*]pyrimidin-6-yl]-2-butynamide (29). A –30 °C stirred solution of 6-amino-4-[(3-chloro-4-fluorophenyl)amino]pyrido[3,4-*d*]pyrimidine²⁹ (**17d**) (0.290 g, 1.0 mmol), 2-butynoic acid (**18b**) (0.092 g,

1.1 mmol), and pyridine (5 mL) was treated with EDCI·HCl (0.242 g, 1.26 mmol). After it was stirred overnight, the dark solution was poured into 40 mL of saturated aqueous NaHCO₃. The formed precipitate was collected, washed with water, and then dissolved in CHCl₃/MeOH (10:1). The solution was purified by column chromatography and was eluted with CHCl₃/MeOH (20:1) to obtain nearly pure product, which was dissolved in MeOH/CH₂Cl₂ (4:1). The solution was clarified with charcoal and concentrated to 5 mL at which point crystallization occurred. The precipitate was collected, washed with MeOH and then ether, and dried to provide **29** (0.04 g, 11%); mp 258–261 °C. ¹H NMR [(CD₃)₂SO] δ: 11.38 (s, 1H), 10.28 (s, 1H), 8.97 (s, 1H), 8.74 (s, 1H), 8.59 (s, 1H), 8.07 (m, 1H), 7.74 (m, 1H), 7.41 (t, *J* = 9 Hz, 1H), 2.02 (s, 3H). APCIMS *m/z* (relative intensity): 356 (M⁺, 100). Anal. (C₁₇H₁₁-ClFN₅O) C, H, N.

N-[4-[(3-Chloro-4-fluorophenyl)amino]pyrido[3,4-*d*]pyrimidin-6-yl]-2-hexynamide (30). A similar reaction of **17d** (0.290 g, 1.0 mmol), 2-hexynoic acid (**18c**) (0.123 g, 1.1 mmol), EDCI·HCl (0.242 g, 1.26 mmol), and pyridine (5 mL) followed by workup and crystallization from EtOAc provided **30** (0.043 g, 11%); mp 233–235 °C. ¹H NMR [(CD₃)₂SO] δ: 11.41 (s, 1H), 10.27 (s, 1H), 8.97 (s, 1H), 8.74 (s, 1H), 8.59 (s, 1H), 8.07 (m, 1H), 7.75 (m, 1H), 7.41 (t, *J* = 9 Hz, 1H), 2.37 (t, *J* = 7 Hz, 2H), 1.53 (q, *J* = 7 Hz, 2H), 0.96 (t, *J* = 7 Hz, 3H). APCIMS *m/z* (relative intensity): 384 (M⁺, 100). Anal. (C₁₉H₁₅ClFN₅O) C, H, N.

N-[4-[(3-Chloro-4-fluorophenyl)amino]pyrido[3,4-*d*]pyrimidin-6-yl]-2-heptynamide (31). A similar reaction of **17d** (0.29 g, 1.0 mmol), 2-heptynoic acid (**18d**) (0.139 g, 1.1 mmol), EDCI·HCl (0.242 g, 1.26 mmol), and pyridine (5 mL) followed by workup, chromatography, and crystallization from EtOAc gave **31** (0.025 g, 6%); mp 220–225 °C. ¹H NMR [(CD₃)₂SO] δ: 11.40 (s, 1H), 10.27 (s, 1H), 8.97 (s, 1H), 8.74 (s, 1H), 8.59 (s, 1H), 8.07 (m, 1H), 7.74 (m, 1H), 7.41 (t, *J* = 9 Hz, 1H), 2.39 (t, *J* = 7 Hz, 2H), 1.49 (m, 2H), 1.39 (m, 2H), 0.86 (t, *J* = 7 Hz, 3H). Anal. (C₂₀H₁₇ClFN₅O) C, H, N.

N-[4-[(3-Chloro-4-fluorophenyl)amino]pyrido[3,4-*d*]pyrimidin-6-yl]-4-(diethylamino)-2-butynamide (32). A similar reaction of **17d** (0.602 g, 2.08 mmol), 4-(diethylamino)-2-butynoic acid³⁴ (**18f**) (0.67 g, 4.16 mmol), EDCI·HCl (1.04 g, 5.41 mmol), and pyridine (5 mL) in CH₂Cl₂ (10 mL), followed by workup and chromatography, gave **32** (0.047 g, 5%); mp 234–236 °C. ¹H NMR [(CD₃)₂SO] δ: 11.52 (s, 1H), 10.26 (s, 1H), 8.97 (s, 1H), 8.75 (s, 1H), 8.60 (s, 1H), 8.07 (m, 1H), 7.75 (m, 1H), 7.41 (t, *J* = 9 Hz, 1H), 3.55 (s, 2H), 2.48 (m, 4H), 0.96 (t, *J* = 7 Hz, 6H). APCIMS *m/z* (relative intensity): 427 (M⁺, 100). Anal. (C₂₁H₂₀ClFN₆O·1.0H₂O) C, H, N.

N-[4-[(3-Chloro-4-fluorophenyl)amino]pyrido[3,4-*d*]pyrimidin-6-yl]-4-(bis(1-methylethyl)amino)-2-butynamide (33). A similar reaction of **17d** (0.580 g, 2.0 mmol), 4-[bis(1-methylethyl)amino]-2-butynoic acid³⁴ (**18g**) (0.440 g, 2.2 mmol), EDCI·HCl (0.480 g, 2.5 mmol), and pyridine (10 mL), followed by workup, chromatography, and crystallization from EtOAc, gave **33** (0.11 g, 12%); mp 200–230 °C (dec). ¹H NMR [(CD₃)₂SO] δ: 11.46 (s, 1H), 10.26 (s, 1H), 8.98 (s, 1H), 8.75 (s, 1H), 8.60 (s, 1H), 8.07 (m, 1H), 7.74 (m, 1H), 7.42 (t, *J* = 9 Hz, 1H), 3.54 (s, 2H), 3.10 (m, 2H), 1.00 (m, 12H). APCIMS *m/z* (relative intensity): 455 (M⁺, 100). Anal. (C₂₃H₂₄ClFN₆O·H₂O) C, H, N.

N-[4-[(3-Chloro-4-fluorophenyl)amino]pyrido[3,4-*d*]pyrimidin-6-yl]-4-(dibutylamino)-2-butynamide (34). A similar reaction of **17d** (0.145 g, 0.5 mmol), 4-(dibutylamino)-2-butynoic acid (**18h**) (0.116 g, 0.55 mmol), EDCI·HCl (0.120 g, 0.63 mmol), and pyridine (2.5 mL), followed by workup, chromatography, and crystallization from EtOAc, gave **34** (0.063 g, 28%); mp 172–174 °C (dec). ¹H NMR [(CD₃)₂SO] δ: 11.56 (s, 1H), 10.30 (s, 1H), 9.02 (s, 1H), 8.79 (s, 1H), 8.64 (s, 1H), 8.10 (m, 1H), 7.81 (m, 1H), 7.46 (t, *J* = 9 Hz, 1H), 3.57 (s, 2H), 2.42 (m, 4H), 1.35 (m, 8H), 0.87 (m, 6H). APCIMS *m/z* (relative intensity): 483 (M⁺, 100). Anal. (C₂₅H₂₈ClFN₆O·0.5H₂O) C, H, N.

N-[4-[(3-Chloro-4-fluorophenyl)amino]pyrido[3,4-*d*]pyrimidin-6-yl]-4-(4-morpholinyl)-2-butynamide (35). A similar reaction of **17d** (0.515 g, 1.78 mmol), 4-(4-morpholinyl)-2-butynoic acid³⁴

(**18i**) (0.445 g, 2.541 mmol), EDCI·HCl (0.633 g, 3.30 mmol), and pyridine (5 mL) in CH₂Cl₂ (10 mL), followed by workup, chromatography, and trituration from CH₂Cl₂/tert-butylmethyl ether provided **35** (0.036 g, 5%); mp 198 °C (dec). ¹H NMR [(CD₃)₂SO] δ: 11.58 (s, 1H), 10.28 (s, 1H), 8.97 (s, 1H), 8.75 (s, 1H), 8.58 (s, 1H), 8.06 (m, 1H), 7.74 (m, 1H), 7.41 (t, *J* = 9 Hz, 1H), 3.56 (m, 4H), 3.49 (s, 2H), 2.45 (m, 4H). APCIMS *m/z* (relative intensity): 441 (M⁺, 100). Anal. (C₂₁H₁₈ClFN₆O₂·0.4CH₂Cl₂·0.3MTBE) C, H, N.

N-[4-[(3-Chloro-4-fluorophenyl)amino]pyrido[3,4-*d*]pyrimidin-6-yl]-5-(4-morpholinyl)-2-pentynamide (36). A similar reaction of **17d** (0.290 g, 1.0 mmol), 5-(4-morpholinyl)-2-pentynoic acid (**18k**) (0.202 g, 1.1 mmol), EDCI·HCl (0.242 g, 1.26 mmol), and pyridine (5 mL), followed by workup, chromatography, and crystallization from EtOAc, gave **36** (0.090 g, 20%); mp 205–209 °C (dec). ¹H NMR [(CD₃)₂SO] δ: 11.45 (s, 1H), 10.32 (s, 1H), 9.01 (s, 1H), 8.78 (s, 1H), 8.63 (s, 1H), 8.11 (m, 1H), 7.80 (m, 1H), 7.45 (t, *J* = 9 Hz, 1H), 3.55 (m, 4H), 2.48 (m, 4H), 2.40 (m, 4H). APCIMS *m/z* (relative intensity): 455 (M⁺, 100). Anal. (C₂₂H₂₀ClFN₆O₂·0.2H₂O) C, H, N.

N-[4-[(3-Bromo-4-fluorophenyl)amino]pyrido[3,4-*d*]pyrimidin-6-yl]-5-(4-morpholinyl)-2-pentynamide (37). A similar reaction of 6-amino-4-[(3-bromo-4-fluorophenyl)amino]pyrido[3,4-*d*]pyrimidine²⁹ (**17e**) (0.334 g, 1.0 mmol), 5-(4-morpholinyl)-2-pentynoic acid (**18k**) (0.202 g, 1.1 mmol), EDCI·HCl (0.242 g, 1.26 mmol), and pyridine (5 mL), followed by workup and chromatography, gave **37** (0.042 g, 8%); mp 190–192 °C (dec). ¹H NMR [(CD₃)₂SO] δ: 11.40 (s, 1H), 10.26 (s, 1H), 8.97 (s, 1H), 8.74 (s, 1H), 8.59 (s, 1H), 8.15 (m, 1H), 7.81 (m, 1H), 7.38 (t, *J* = 9 Hz, 1H), 3.52 (m, 4H), 2.55 (m, 4H), 2.38 (m, 4H). APCIMS *m/z* (relative intensity): 501 (⁸¹BrMH⁺, 100). Anal. (C₂₂H₂₀-BrFN₆O₂·0.3CHCl₃) C, H, N.

N-[4-[(3-Chloro-4-fluorophenyl)amino]pyrido[3,4-*d*]pyrimidin-6-yl]-5-(1-piperidinyl)-2-pentynamide (38). A similar reaction of **17d** (4.70 g, 16.2 mmol), 5-(1-piperidinyl)-2-pentynoic acid, lithium salt (**18l**) (6.03 g, 32.2 mmol), pyridine hydrochloride (4.62 g, 40 mmol), EDCI·HCl (7.70 g, 40 mmol), and pyridine (80 mL), followed by workup, chromatography, and crystallization from EtOAc, gave **38** (0.35 g, 5%); mp 290–300 °C (dec). ¹H NMR [(CD₃)₂SO] δ: 11.40 (s, 1H), 10.27 (s, 1H), 8.97 (s, 1H), 8.74 (s, 1H), 8.59 (s, 1H), 8.07 (m, 1H), 7.74 (m, 1H), 7.42 (t, *J* = 9 Hz, 1H), 2.52 (m, 2H), 2.50 (m, 2H), 2.33 (m, 4H), 1.43 (m, 4H), 1.31 (m, 2H). APCIMS *m/z* (relative intensity): 453 (M⁺, 100). Anal. (C₂₃H₂₂ClFN₆O·H₂O) C, H, N.

N-[4-[(3-Chloro-4-fluorophenyl)amino]pyrido[3,4-*d*]pyrimidin-6-yl]-5-(4-methyl-1-piperazinyl)-2-pentynamide (39). A similar reaction of **17d** (2.35 g, 8.1 mmol), 5-(4-methyl-1-piperazinyl)-2-pentynoic acid, lithium salt (**18m**) (3.49 g, 16 mmol), pyridine hydrochloride (2.31 g, 20 mmol), EDCI·HCl (3.85 g, 20 mmol), and pyridine (40 mL), followed by workup, chromatography, and crystallization from EtOAc, gave **39** (0.78 g, 20%); mp 170–180 °C. ¹H NMR (CD₃OD) δ: 8.93 (s, 1H), 8.71 (s, 1H), 8.57 (s, 1H), 8.05 (m, 1H), 7.70 (m, 1H), 7.26 (t, *J* = 9 Hz, 1H), 2.68 (m, 4H), 2.55 (br m, 8H), 2.28 (s, 3H). APCIMS *m/z* (relative intensity): 468 (M⁺, 100). Anal. (C₂₃H₂₃ClFN₇O·0.5H₂O) C, H, N.

N-[4-[(3-Bromo-4-fluorophenyl)amino]pyrido[3,4-*d*]pyrimidin-6-yl]-5-(4-methyl-1-piperazinyl)-2-pentynamide (40). A similar reaction of **17e** (0.334 g, 1.0 mmol), 5-(4-methyl-1-piperazinyl)-2-pentynoic acid (**18m**) (0.216 g, 1.1 mmol), EDCI·HCl (0.242 g, 1.3 mmol), and pyridine (5 mL), followed by workup, chromatography, and crystallization from EtOAc, gave **40** (0.027 g, 5%); mp 190–195 °C. ¹H NMR (CD₃OD) δ: 8.96 (s, 1H), 8.73 (s, 1H), 8.59 (s, 1H), 8.10 (m, 1H), 7.78 (m, 1H), 7.26 (t, *J* = 9 Hz, 1H), 2.68 (m, 4H), 2.55 (br m, 8H), 2.30 (s, 3H). APCIMS *m/z* (relative intensity): 514 (⁸¹BrMH⁺, 100). Anal. (C₂₃H₂₃BrFN₇O·0.8H₂O) C, H, N. Alternatively, a similar reaction of **17e** (0.538 g, 1.61 mmol), 5-(4-methyl-1-piperazinyl)-2-pentynoic acid, lithium salt (**18m**) (0.697 g, 3.22 mmol), pyridine hydrochloride (0.462 g, 4.00 mmol), EDCI·HCl (0.770 g, 4.0 mmol), and pyridine (8 mL) provided pure **40** (35% yield). Anal. (C₂₃H₂₃BrFN₇O·H₂O) C, H, N.

Synthesis of 5-(Aminosubstituted)-2-pentynoic Acids. 5-(1-Piperidinyl)-2-pentynoic Acid (18i). 1-(3-Butynyl)piperidine (**42**; R₁, R₂ = piperidinyl) was synthesized as previously reported.⁴⁵ ¹H NMR (CDCl₃) δ: 1.38 (ddd, *J* = 11.3, 6.0, 5.8 Hz, 2H), 1.54 (dt, *J* = 11.3, 5.8 Hz, 4H), 1.92 (t, *J* = 2.7, Hz, 1H), 2.34 (m, 6H), 2.53 (m, 2H).

A stirred -78°C solution of **42** (R₁, R₂ = piperidinyl) (2.56 g, 18.7 mmol) in ether (65 mL) was treated with *n*-BuLi (2.3 mL of a 10 M solution in hexanes). After 3 h at -78°C , powdered CO₂ was added to bring the solution volume to ca. 250 mL while maintaining the temperature at -78°C . The cooling bath was removed, and the mixture was stirred until all excess CO₂ had evaporated (ca. 16 h). The resultant lithium salt was collected by filtration and then dissolved in 30 mL of water. The solution was adjusted to pH 5 with 5% aq HCl and then loaded onto a column of 29 g of Dowex 50X8-200 ion-exchange resin (H⁺ form, prewashed with 800 mL of deionized water). The column was eluted with ca. 2 column volumes of water and then with 500 mL of 0.2 N aq NH₄OH, while 8 mL fractions were collected. The fractions containing product were pooled and concentrated under reduced pressure to leave a residue that was coevaporated twice with MeOH to leave **18i** (2.42 g, 72%) as a light orange solid, which was utilized without further processing. ¹H NMR [(CD₃)₂SO] δ: 1.28 (m, 1H), 1.58 (m, 1H), 1.65 (m, 4H), 2.82 (m, 2H), 2.91 (t, *J* = 7.5 Hz, 2H), 3.17 (t, *J* = 7.5 Hz, 2H), 3.33 (d, *J* = 12.2 Hz, 2H).

5-(4-Methyl-1-piperazinyl)-2-pentynoic Acid (18m). Utilizing a method similar to that of Turner et al.,⁴⁶ we stirred a mixture of 4-(tosyloxy)-1-butyne (**41**) (8.80 g, 40 mmol), *N*-methylpiperazine (8.02 g, 80 mmol), dry, powdered K₂CO₃ (25 g), and DMF (25 mL) overnight at room temperature. Ether (100 mL) was added, the mixture was filtered, and the filter cake was washed with ether. The filtrate was concentrated at 20 mm and 40 °C to remove ether and most of the DMF, and residual DMF was removed by silica gel chromatography and eluted sequentially with CHCl₃/hexanes (1:1), then CHCl₃ (to remove DMF), and finally CHCl₃/MeOH (10:1) to strip off the product. Concentration of product fractions provided **42** (R₁, R₂ = 4-methyl-1-piperazinyl) (3.78 g, 62%) as an oil, which was utilized without further processing. ¹H NMR (D₂O) δ: 2.38 (t, *J* = 7 Hz, 2H), 2.19 (t, *J* = 7 Hz, 2H), 2.06 (s, 1H), 2.01 (s, 3H), 1.9–2.7 (br m, 8H). APCIMS *m/z* (relative intensity): 153 (MH⁺, 100).

A stirred -78°C solution of **42** (R₁, R₂ = 4-methyl-1-piperazinyl) (1.06 g, 7 mmol) in dry THF (15 mL) was treated with *n*-BuLi (5.0 mL of 1.6 M solution in hexane). The mixture was stirred for 1 h at -78°C , and then dry CO₂ gas was bubbled in at a moderate rate at -78°C for 1 h and then while allowing the mixture to warm to room temperature. After further stirring for 1 h at room temperature, the solution was ice-cooled and treated with 1 N aq HCl (8 mL). The mixture was concentrated, and the residue was coevaporated with absolute EtOH (2 × 25 mL). The resulting sticky solid was dissolved in hot absolute EtOH (15 mL), and ether (4 mL) was added to precipitate a solid. The solid, free of LiCl, was collected and then recrystallized by dissolution in warm water (1 mL) followed by addition of MeCN (3 mL). The product was collected, washed with MeCN (1 mL) and ether, and dried to give **18m** (0.97 g, 67%); mp 207–209 °C (dec). ¹H NMR (CD₃-OD) δ: 3.2 (br m, 4H), 2.8–3.0 (br m, 4H), 2.80 (s, 3H), 2.76 (t, *J* = 7 Hz, 2H), 2.52 (t, *J* = 7 Hz, 2H). APCIMS *m/z* (relative intensity): 197 (MH⁺, 100). Anal. (C₁₀H₁₆N₂O₂·0.6H₂O) C, H, N.

5-(4-Methyl-1-piperazinyl)-2-pentynoic Acid, Lithium Salt (18m). A stirred -65°C solution of **42** (R₁, R₂ = 4-methyl-1-piperazinyl) (50 g, 0.33 mol) and dry THF (155 mL) was treated with *n*-BuLi (135 g of a 1.6 M solution in hexanes) followed by dry CO₂ (15 g, 395 mmol). The mixture was stirred at -65°C for ca. 3 h, warmed to 25 °C, and then diluted with 110 mL of isopropyl alcohol and 10 mL of water. After warming to reflux, the solution was cooled to allow crystallization, and then the product was collected by filtration and vacuum-dried at ca. 65 °C to give **18m**, lithium salt (50 g, 75%) hydrated with ≤2% water.

5-(Diethylamino)-2-pentynoic Acid (18j). A similar reaction of *n*-BuLi (2.7 mL of a 2.18 M solution in THF), 4-(diethylamino)-

1-butyne⁴⁷ (**42**; R₁ = R₂ = ethyl) (0.816 g, 6.5 mmol), and THF (20 mL) at -78°C , followed by carboxylation and workup, gave **18j** as a light yellow solid (0.652 g, 59% yield), which was utilized directly without further processing. ¹H NMR [(CD₃)₂SO] δ: 3.79 (br, 1H), 2.85 (t, *J* = 7.3 Hz, 2H), 2.74 (q, *J* = 7.0, 5.0 Hz, 4H), 2.52–2.4 (m, 2H), 1.03 (t, *J* = 7.2 Hz, 6H). APCIMS *m/z* (relative intensity): 170 (MH⁺, 100).

5-(4-Morpholinyl)-2-pentynoic Acid (18k). A similar reaction of *n*-BuLi (15 mL of a 2.18 M solution in THF), 4-(3-butynyl)-morpholine³⁰ (**42**; R₁, R₂ = morpholinyl) (5.06 g, 36 mmol), and THF (100 mL), followed by carboxylation and workup, gave **18k** as a dull yellow solid (5.08 g, 77%), which was used directly without further processing. ¹H NMR [(CD₃)₂SO] δ: 7.2–7.4 (br, 1H), 3.54 (m, 4H), 2.49–2.36 (m, 8H). APCIMS *m/z* (relative intensity): 184 (MH⁺, 100).

ELISA-Based erbB Kinase Assay. The erbB1, erbB2, and erbB4 cytoplasmic fusion proteins were made by cloning the erbB1 sequence (Met-668 to Ala-1211), erbB2 (Ile-675 to Val-1256), and erbB4 sequence (Gly-259 to Gly-690) into the baculoviral vector pFastBac using PCR. Proteins were expressed in baculovirus-infected Sf9 insect cells as GST fusion proteins. The proteins were purified by affinity chromatography using glutathione sepharose beads. Inhibition of erbB tyrosine kinase activity was assessed using an ELISA-based receptor tyrosine kinase assay. Kinase reactions (50 mM HEPES, pH 7.4, 125 mM NaCl, 10 mM MgCl₂, 100 μM sodium orthovanadate, 2 mM dithiothreitol, 20 μM ATP, test compound or vehicle control, and 1–5 nM GST-erbB per 50 μL of reaction mixture) were run in 96-well plates coated with 0.25 mg/mL poly-Glu-Tyr (Sigma). The reactions were incubated for 6 min at room temperature while being shaken. Kinase reactions were stopped by removal of the reaction mixture, then the wells were washed with wash buffer (0.1% Tween 20 in PBS). Phosphorylated tyrosine residues were detected by adding 0.2 μg/mL anti-phosphotyrosine antibody (Oncogene Ab-4; 50 μL/well) coupled to horseradish peroxidase (HRP) diluted in PBS containing 3% BSA and 0.05% Tween 20 for 25 min while being shaken at room temperature. The antibody was removed, and plates were washed in wash buffer. HRP substrate (SureBlue3,3',5,5'-tetramethyl benzidine or TMB, Kirkegaard & Perry Labs) was added (50 μL per well) and incubated for 10–20 min while it was shaken at room temperature. The TMB reaction was stopped with the addition of 50 μL of stop solution (0.09 N H₂SO₄). The signal was quantified by measuring absorbance at 450 nm. IC₅₀ values were determined for test compounds using the median effect method.⁴⁸

Inhibition of erbB1 and erbB2 Autophosphorylation in Cells Using BioVeris Technology. Inhibition of erbB1 tyrosine kinase activity was evaluated in NIH3T3 cells transfected with the full-length human erbB1 receptor, and inhibition of erbB2 tyrosine kinase activity was evaluated in T24 NIH 3T3 cells transfected with a chimeric receptor with the extracellular binding domain of erbB1 and the intracellular kinase domain of erbB2. The derivation of these lines has been previously described by Cohen et al.⁴⁹ Cells were plated in a 96-well plate at a density of 20 000 cells per well in DMEM/F12 media (Gibco BRL) containing 10% fetal bovine serum (Gibco, BRL) and 10 ng/mL Gentamicin (Gibco, BRL). Cells were cultured at 37 °C in 5% CO₂. Prior to drug treatment, the cells were cultured in serum-free medium for 12–24 h. The cells were then treated with the test compound dissolved in DMSO for 2 h (final DMSO concentration of <0.5%) at 37 °C and 5% CO₂. After the 2 h drug treatment, the cells were stimulated with 100 ng/mL EGF (Sigma) for 10 min at 37 °C and 5% CO₂. The medium was removed, and the cells were immediately lysed in buffer (50 mM HEPES pH 7.5, 150 mM NaCl, 10% glycerol, 1 mM EDTA, 1% Triton, 10 mM β-glycerophosphate, 0.1 mM NaVa, 1 mM NaF, 0.25% deoxycholic acid, 10 μg/mL aprotinin, 10 μg/mL leupeptin) for 15 min at room temperature, mixing gently.

Inhibition of erbB1 autophosphorylation was detected using BioVeris technology. Anti-erbB1 antibody tagged with biotin was added to the lysates to capture erbB1 (NeoMarkers Clone 528; 100 ng/mL per well). An antiphospho-erbB1 antibody (Cell Signaling p-Y1068; 100 ng/mL per well) labeled with ruthenium (BioVeris)

was simultaneously added to detect phosphorylated erbB1. Plates were mixed gently for 60 min at room temperature. Magnetic beads coated with streptavidin (Dynabeads M 289 streptavidin, Dynal Biotech Inc.) were added at a final concentration of 50 ng/mL and mixed gently at room temperature for 30 min. The antibodies and beads were diluted in the following buffer: 150 mM NaCl, 50 mM Tris-HCl pH 7.4, 1% BSA, 0.02% Na azide. After the incubation, samples were analyzed using a BioVeris M8 analyzer. IC₅₀ determinations were determined using the median effect method.

Inhibition of erbB2 autophosphorylation was also detected using BioVeris technology. Anti-erbB1 tagged with biotin was added to the lysate to capture erbB1/erbB2 chimeric protein (NeoMarkers Clone 528; 200 ng/mL per well). An antiphospho-erbB2 antibody (Cell Signaling p-Y1248, 200 ng/mL per well) labeled with ruthenium (BioVeris) was simultaneously added to detect phosphorylated erbB2. The remaining methods followed procedures outlined for inhibition of erbB1 autophosphorylation.

Inhibition of EGF and Heregulin-Stimulated erbB Autophosphorylation in Cells Using Western Blotting. Inhibition of EGF-stimulated or heregulin-stimulated erbB receptor autophosphorylation was assessed in either NIH 3T3 fibroblasts expressing full length human erbB1, the T24 NIH 3T3 fibroblasts expressing a chimeric receptor with the extracellular binding domain of erbB1 and the intracellular kinase domain of erbB2, or the human breast carcinoma cell line MDA-MB-453 by antiphosphotyrosine Western blots. Western blotting procedures have been previously described.⁵⁰ To detect phospho-erbB1, an antiphospho-erbB1 antibody was used (p-Y1068, Cell Signaling). To detect phospho-erbB2, an antiphospho-erbB2 antibody was used (p-Y1248, Cell Signaling). To detect phospho-erbB signals in MDA-MB-453 cells, an antiphospho-Tyr antibody was used as described.⁵⁰ Band intensities from the antiphosphotyrosine Western blots were determined using a Molecular Dynamics laser densitometer and expressed as percent control. IC₅₀ determinations were determined using the median effect method.

Pharmacokinetics. All animals were fasted overnight prior to dosing the next morning, and food was withheld until 4 h following dosing. Water was allowed ad libitum throughout the study. For each study, blood samples were collected from a jugular cannula into EDTA/ascorbic acid tubes. Sampling occurred prior to dosing and at 7–9 different time points up to 24 h after the iv and the po dose. Plasma drug concentration was determined by a LC/MS/MS assay. Briefly, **39** was isolated from plasma using protein precipitation with acetonitrile. Supernatant was injected directly into an amide column with mobile phase consisting of acetonitrile/10 mM ammonium formate (pH = 4.0) (35:65, v/v), with mass spectrometric detection. Drug concentration below the limit of quantitation (<6.5 ng/mL) was treated as zero for pharmacokinetic and statistical calculations.

In Vivo Antitumor Effects of 39. Immune-deficient CB.17 SCID mice and nude mice (NCR nu/nu) were purchased from Charles River. Mice were housed in microisolator cages within a barrier facility on a 12 h light/dark cycle and received food and water ad libitum. Animal housing was in accord with AAALAC guidelines. All experimental protocols involving animals were approved by the institutional animal care and use committee. The A431 epidermoid carcinoma, the H125 non-small-cell lung carcinoma line, and the SKOV3 ovarian carcinoma line were maintained by serial passage in nude mice (NCR nu/nu). The SF-767 glioblastoma and the BxPC-3 pancreatic tumor lines were maintained by serial passage in SCID mice.

Tumors were implanted subcutaneously in immune-deficient mice and allowed to grow to a size of 100–150 mg before dosing was initiated. The drug was dissolved in 0.05 N Na lactate buffer, pH 4.0, and the route of drug administration for all studies was oral. Animals were dosed either daily for 14 days or daily 5 days a week for 2–3 weeks. Tumor measurements were made 2–3 times per week until tumors reached 750 mg. Efficacy was assessed by tumor growth delay (T-C) and tumor growth delay index (GDI). Tumor growth delay is the difference, in days, for the treated (T) and control (C) tumors to reach 750 mg. Calculation of tumor growth delay (T-C) was performed as described previously.^{51–54}

Efficacy was also assessed by calculating the growth delay index (GDI), which allows for a better comparison of the magnitude of tumor growth suppression between studies since it factors in differences in dosing schedules. GDI is calculated by dividing the T-C by the number of treatment days and multiplying by 100%. A GDI of 0 indicates no effect; a GDI below 100 indicates a slowing of tumor growth, but growth is still occurring during treatment. A GDI of 100 would mean complete tumor stasis, and a GDI above 100 means that drug treatment delayed tumor growth for longer than the duration of treatment. Compound **39** was considered to have activity if it could produce a GDI of greater than 50.

Acknowledgment. This work was partially supported by the Auckland Division of the Cancer Society of New Zealand. The T24 NIH 3T3 lines were a gift from Dr. Bruce Cohen at the National Cancer Institute, Bethesda, MD.

Supporting Information Available: Combustion analytical data. This material is available free of charge via the Internet at <http://pubs.acs.org>.

References

- (1) Lemmon, M. A. The EGF receptor family as therapeutic targets in breast cancer. *Breast Dis.* **2003**, *18*, 33–43.
- (2) Ang, K. K.; Andratschke, N. H.; Milas, L. Epidermal growth factor receptor and response of head-and-neck carcinoma to therapy. *Int. J. Radiat. Oncol., Biol., Phys.* **2004**, *58*, 959–965.
- (3) Meert, A. P.; Martin, B.; Paesmans, M.; Berghmans, T.; Mascaux, C.; Verdebout, J.-M.; Delmotte, P.; Lafitte, J.-J.; Sculier, J.-P. The Role of HER-2/neu expression on the survival of patients with lung cancer: a systematic review of the literature. *Br. J. Cancer* **2003**, *89*, 959–965.
- (4) Hynes, N. E.; Lane, H. A. ErbB receptors and cancer: The complexity of targeted inhibitors. *Nat. Rev. Cancer* **2005**, *5*, 341–354.
- (5) Denny, W. A. The 4-anilinoquinazoline class of inhibitors of the erbB family of receptor tyrosine kinases. *Farmacology* **2001**, *56*, 51–56.
- (6) Cockerill, S.; Stubberfield, C.; Stables, J.; Carter, M.; Guntrip, S.; Smith, K.; McKeown, S.; Shaw, R.; Topley, P.; Thomsen, L.; Affleck, K.; Jowett, A.; Hayes, D.; Willson, M.; Woollard, P.; Spalding, D. Indazolylamino quinazolines and pyridopyrimidines as inhibitors of the EGFR and c-erbB-2. *Bioorg. Med. Chem. Lett.* **2001**, *11*, 1401–1405.
- (7) Palmer, B. D.; Trumpp-Kallmeyer, S.; Fry, D. W.; Nelson, J. M.; Showalter, H. D. H.; Denny, W. A. Tyrosine kinase inhibitors. 11. Soluble analogues of pyrrolo- and pyrazinoquinazolines as EGFR inhibitors: synthesis, biological evaluation, and modelling of the mode of binding. *J. Med. Chem.* **1997**, *40*, 1519–1529.
- (8) Vansteenkiste, J. F. Gefitinib (Iressa): a novel treatment for non-small-cell lung cancer. *Expert Rev. Anticancer Ther.* **2004**, *4*, 5–17.
- (9) Tiseo, M.; Loprevite, M.; Ardizzoni, A. Epidermal growth factor receptor inhibitors: a new perspective in the treatment of lung cancer. *Curr. Med. Chem: Anti-Cancer Agents* **2004**, *4*, 139–148.
- (10) Bonomi, P. Erlotinib: a new therapeutic approach for non-small-cell lung cancer. *Expert Opin. Invest. Drugs* **2003**, *12*, 1395–1401.
- (11) Lynch, T. J.; Bell, D. W.; Sordella, R.; Gurubhagavatula, S.; Okimoto, R. A.; Brannigan, B. W.; Harris, P. L.; Haserlat, S. M.; Supko, J. G.; Haluska, F. G.; Louis, D. N.; Christiani, D. C.; Settleman, J.; Haber, D. A. Activating mutations in the epidermal growth factor receptor underlying responsiveness of non-small-cell lung cancer to gefitinib. *N. Engl. J. Med.* **2004**, *350*, 2129–2139.
- (12) Paez, J. G.; Jaenke, P. A.; Lee, J. C.; Tracy, S.; Greulich, H.; Gabriel, S.; Herman, P.; Kaye, F. J.; Lindeman, N.; Boggon, T. J.; Naoki, K.; Sasaki, H.; Fujii, Y.; Eck, M. J.; Sellers, W. R.; Johnson, B. E.; Meyerson, M. EGFR mutations in lung cancer: Correlation with clinical response to gefitinib therapy. *Science* **2004**, *304*, 1497–1500.
- (13) Pao, W.; Miller, V.; Zakowski, M.; Doherty, J.; Politi, K.; Sarkaria, I.; Singh, B.; Heelan, R.; Rusch, V.; Fulton, L.; Mardis, E.; Kupfer, D.; Wilson, R.; Kris, M.; Varmus, H. EGF receptor gene mutations are common in lung cancers from “never smokers” and are associated with sensitivity of tumors to gefitinib and erlotinib. *Proc. Natl. Acad. Sci. U.S.A.* **2004**, *101*, 13306–13311.
- (14) Fabian, M. A.; Biggs, W. H., III; Treiber, D. K.; Atteridge, C. E.; Azimioara, M. D.; Benedetti, M. G.; Carter, T. A.; Ciceri, P.; Edeen, P. T.; Floyd, M.; Ford, J. M.; Galvin, M.; Gerlach, J. L.; Grotzfeld, R. M.; Herrgard, S.; Insko, D. E.; Insko, M. A.; Lai, A. G.; Lelias, J.-M.; Mehta, S. A.; Milanov, Z. V.; Velasco, A. M.; Wodicka, L. M.; Patel, H. K.; Zarrinkar, P. P.; Lockhart, D. J. A small molecule-kinase interaction map for clinical kinase inhibitors. *Nat. Biotechnol.* **2005**, *23*, 329–336.

- (15) Sordella, R.; Bell, D. W.; Haber, D. A.; Settleman, J. Gefitinib-sensitizing mutations in lung cancer activate anti-apoptotic pathways. *Science* **2004**, *305*, 1163–1167.
- (16) Kobayashi, S.; Boggon, T. J.; Dayaram, T.; Janne, P. A.; Kocher, O.; Meyerson, M.; Johnson, B. E.; Eck, M. J.; Tenen, D. G.; Halmos, B. EGFR mutation and resistance of non-small-cell lung cancer to gefitinib. *N. Engl. J. Med.* **2005**, *352*, 786–792.
- (17) Pao, W.; Miller, V. A.; Politi, K. A.; Riely, G. J.; Somwar, R.; Zakowski, M. F.; Kris, M. G.; Varmus, H. Acquired resistance of lung adenocarcinomas to gefitinib or erlotinib is associated with a second mutation in the EGFR kinase domain. *PLoS Med.* **2005**, *2*, 225–235.
- (18) Rusnak, D. W.; Lackey, K.; Affleck, K.; Wood, E. R.; Alligood, K. J.; Rhodes, N.; Keith, B. R.; Murray, D. M.; Knight, W. B.; Mullin, R. J.; Gilmer, T. M. The effects of the novel, reversible epidermal growth factor receptor/erbB-2 tyrosine kinase inhibitor, GW572016, on the growth of human normal and tumor-derived cell lines in vitro and in vivo. *Mol. Cancer Ther.* **2001**, *1*, 85–94.
- (19) Wood, E. R.; Truesdale, A. T.; McDonald, O. B.; Yuan, D.; Hassell, A.; Dickerson, S. H.; Ellis, B.; Pennisi, C.; Horne, E.; Lackey, K.; Alligood, K. J.; Rusnak, D. W.; Gilmer, T. M.; Shewchuk, L. A unique structure for epidermal growth factor receptor bound to GW572016 (lapatinib): Relationships among protein conformation, inhibitor off-rate, and receptor activity in tumor cells. *Cancer Res.* **2004**, *64*, 6652–6659.
- (20) Vite, G. D.; Gavai, A. V.; Fink, B. E.; Mastalerz, H.; Kadow, J. F. Preparation of C-6 Modified Indazolyl Pyrrolotriazines as Antiproliferative Agents. PCT Int. Appl. WO 2004054514 A2, 2004; 81 pp.
- (21) Borman, S. Hopes ride on drug candidates. Researchers reveal potential new medicines for thrombosis, anxiety, diabetes, and cancer. *Chem. Eng. News* **2005**, *83*, 40–44.
- (22) Mellinghoff, I. K.; Tran, C.; Sawyers, C. L. Growth Inhibitory effects of the dual ErbB1/ErbB2 Tyr kinase inhibitor PKI-166 on human prostate cancer xenografts. *Cancer Res.* **2002**, *62*, 5254–5259.
- (23) Traxler, P.; Allegrini, P. R.; Brandt, R.; Brueggen, J.; Cozens, R.; Fabbro, D.; Grosios, K.; Lane, H. A.; McSheehy, P.; Mestan, J.; Meyer, T.; Tang, C.; Wartmann, M.; Wood, J.; Caravatti, G. AEE788: A dual family epidermal growth factor receptor/erbB2 and vascular endothelial growth factor receptor tyrosine kinase inhibitor with antitumor and antiangiogenic activity. *Cancer Res.* **2004**, *64*, 4931–4941.
- (24) Stamos, J.; Sliwkowski, M. X.; Eigenbrot, C. Structure of the epidermal growth factor receptor kinase domain alone and in complex with a 4-anilinoquinazoline inhibitor. *J. Biol. Chem.* **2002**, *277*, 46265–46272.
- (25) Shewchuk, L.; Hassell, A.; Wisely, B.; Rocque, W.; Holmes, W.; Veal, J.; Kuyper, L. F. Binding mode of the 4-anilinoquinazoline class of protein kinase inhibitor: X-ray Crystallographic studies of 4-anilinoquinazolines bound to cyclin-dependent kinase 2 and p38 kinase. *J. Med. Chem.* **2000**, *43*, 133–138.
- (26) Wissner, A.; Berger, D. M.; Boschelli, D. H.; Floyd, M. B.; Greenberger, L. M.; Gruber, B. C.; Johnson, B. D.; Mamuya, N.; Nilakantan, R.; Reich, M. F.; Shen, R.; Tsou, H. R.; Upešlacis, E.; Wang, Y. F.; Wu, B.; Ye, F.; Zhang, N. 4-Anilino-6,7-dialkoxyquinoline-3-carbonitrile inhibitors of epidermal growth factor receptor kinase and their bioisosteric relationship to the 4-anilino-6,7-dialkoxyquinazoline inhibitors. *J. Med. Chem.* **2000**, *43*, 3244–3256.
- (27) Singh, J.; Dobrusin, E. M.; Fry, D. W.; Haske, T.; Whitty, A.; McNamara, D. J. Structure-based design of a potent, selective, and irreversible inhibitor of the catalytic domain of the erbB receptor subfamily of protein tyrosine kinases. *J. Med. Chem.* **1997**, *40*, 1130–1135.
- (28) Fry, D. W.; Bridges, A. J.; Denny, W. A.; Doherty, A.; Greis, K. D.; Hicks, J. L.; Hook, K. E.; Keller, P. R.; Leopold, W. R.; Loo, J. A.; McNamara, D. J.; Nelson, J. M.; Sherwood, V.; Smaill, J. B.; Trumpp-Kallmeyer, S.; Dobrusin, E. M. Specific, irreversible inactivation of the epidermal growth factor receptor and erbB2, by a new class of tyrosine kinase inhibitor. *Proc. Natl. Acad. Sci. U.S.A.* **1998**, *95*, 12022–12027.
- (29) Smaill, J. B.; Palmer, B. D.; Rewcastle, G. W.; Denny, W. A.; McNamara, D. J.; Dobrusin, E. M.; Bridges, A. J.; Zhou, H.; Showalter, H. D. H.; Winters, R. T.; Leopold, W. R.; Fry, D. W.; Nelson, J. M.; Slintak, V.; Elliott, W. L.; Roberts, B. J.; Vincent, P. W.; Patmore, S. J. Tyrosine kinase inhibitors. 15. 4-(Phenylamino)-quinazoline and 4-(phenylamino)pyrido[d]pyrimidine acrylamides as irreversible inhibitors of the ATP binding site of the epidermal growth factor receptor. *J. Med. Chem.* **1999**, *42*, 1803–1815.
- (30) Smaill, J. B.; Rewcastle, G. W.; Bridges, A. J.; Zhou, H.; Showalter, H. D. H.; Fry, D. W.; Nelson, J. M.; Sherwood, V.; Elliott, W. L.; Vincent, P. W.; DeJohn, D.; Loo, J. A.; Gries, K. D.; Chan, O. H.; Reyner, E. L.; Lipka, E.; Denny, W. A. Tyrosine kinase inhibitors. 17. Irreversible inhibitors of the epidermal growth factor receptor: 4-(phenylamino)quinazoline- and 4-(phenylamino)pyrido[3,2-d]pyrimidine-6-acrylamides bearing additional solubilizing functions. *J. Med. Chem.* **2000**, *43*, 1380–1397.
- (31) Allen, L. F.; Eiseman, I. A.; Fry, D. W.; Lenehan, P. F. CI-1033, an irreversible pan-erbB receptor inhibitor and its potential application for the treatment of breast cancer. *Semin. Oncol.* **2003**, *30* (Suppl. 16), 65–78.
- (32) Calvo, E.; Tolcher, A. W.; Hammond, L. A.; Patnaik, A.; de Bono, J. S.; Eiseman, I. A.; Olson, S. C.; Lenehan, P. F.; McCreery, H.; LoRusso, P.; Rowinsky, E. K. Administration of CI-1033, an irreversible pan-erbB tyrosine kinase inhibitor, is feasible on a 7-day on, 7-day off schedule: a phase I pharmacokinetic and food effect study. *Clin. Cancer Res.* **2004**, *10*, 7112–7120.
- (33) Smaill, J. B.; Showalter, H. D. H.; Zhou, H.; Bridges, A. J.; McNamara, D. J.; Fry, D. W.; Nelson, J. M.; Sherwood, V.; Vincent, P. W.; Roberts, B. J.; Elliott, W. L.; Denny, W. A. Tyrosine kinase inhibitors. 18. 6-Substituted 4-anilinoquinazolines and 4-anilino-pyrido[3,4-d]pyrimidines as soluble, irreversible inhibitors of the epidermal growth factor receptor. *J. Med. Chem.* **2001**, *44*, 429–440.
- (34) Tsou, H. R.; Mamuya, N.; Johnson, B. D.; Reich, M. F.; Gruber, B. C.; Ye, F.; Nilakantan, R.; Shen, R.; Discifani, C.; DeBlanc, R.; Davis, R.; Koehn, F. E.; Greenberger, L. M.; Wang, Y. F.; Wissner, A. 6-Substituted-4-(3-bromophenylamino)quinazolines as putative irreversible inhibitors of the epidermal growth factor receptor (EGFR) and human epidermal growth factor receptor (HER-2) tyrosine kinases with enhanced antitumor activity. *J. Med. Chem.* **2001**, *44*, 2719–2734.
- (35) Discifani, C. M.; Carroll, M. L.; Floyd, M. B.; Hollander, I. J.; Husain, Z.; Johnson, B. D.; Kitchen, D.; May, M. K.; Malo, M. S.; Minnick, A. A.; Nilakantan, R.; Shen, R.; Wang, Y.-F.; Wissner, A.; Greenberger, L. M. Irreversible inhibition of epidermal growth factor receptor tyrosine kinase with in vivo activity by N-[4-(3-bromophenylamino)-6-quinazolyl]-2-butynamide (CL-387, 785). *Biochem. Pharmacol.* **1999**, *57*, 917–925.
- (36) Wissner, A.; Overbeek, E.; Reich, M. F.; Brawner Floyd, M.; Johnson, B. D.; Mamuya, N.; Rosfjord, E. C.; Discifani, C.; Davis, R.; Shi, X.; Rabindran, S. K.; Gruber, B. C.; Ye, F.; Hallett, W. A.; Nilakantan, R.; Shen, R.; Wang, Y.-F.; Greenberger, L. M.; Tsou, H.-R. Synthesis and structure–activity relationships of 6,7-disubstituted 4-anilinoquinoline-3-carbonitriles. The design of an orally active, irreversible inhibitor of the tyrosine kinase activity of the epidermal growth factor receptor (EGFR) and the human epidermal growth factor receptor-2 (HER-2). *J. Med. Chem.* **2003**, *46*, 49–63.
- (37) Nunes, M.; Shi, C.; Greenberger, L. M. Phosphorylation of extracellular signal-regulated kinase 1 and 2, protein kinase B, and signal transducer and activator of transcription 3 are differentially inhibited by an epidermal growth factor receptor inhibitor, EKB-569, in tumor cells and normal human keratinocytes. *Mol. Cancer Ther.* **2004**, *3*, 21–27.
- (38) Wissner, A.; Hamann, P. R.; Nilakantan, R.; Greenberger, L. M.; Ye, F.; Rapuano, T. A.; Loganzo, F. Syntheses and EGFR kinase inhibitory activity of 6-substituted-4-anilino [1,7] and [1,8] naphthyridine-3-carbonitriles. *Bioorg. Med. Chem. Lett.* **2004**, *14*, 1411–1416.
- (39) Tsou, H.-R.; Overbeek-Klumpers, E. G.; Hallett, W. A.; Reich, M. F.; Brawner Floyd, M.; Johnson, B. D.; Michalak, R. S.; Nilakantan, R.; Discifani, C.; Golas, J.; Rabindran, S. K.; Shen, R.; Shi, X.; Wang, Y.-F.; Upešlacis, J.; Wissner, A. Optimization of 6,7-disubstituted-4-(aryl amino)quinoline-3-carbonitriles as orally active, irreversible inhibitors of human epidermal growth factor receptor-2 kinase activity. *J. Med. Chem.* **2005**, *48*, 1107–1131.
- (40) Kwak, E. L.; Sordella, R.; Bell, D. W.; Godin-Heymann, N.; Okimoto, R. A.; Brannigan, B. W.; Harris, P. L.; Driscoll, D. R.; Fidias, P.; Lynch, T. J.; Rabindran, S. K.; McGinnis, J. P.; Wissner, A.; Sharma, S. V.; Isselbacher, K. J.; Settleman, J.; Haber, D. A. Irreversible inhibitors of the EGF receptor may circumvent acquired resistance to gefitinib. *Proc. Natl. Acad. Sci. U.S.A.* **2005**, *102*, 7665–7670.
- (41) Rewcastle, G. W.; Denny, W. A.; Bridges, A. J.; Zhou, H.; Cody, D. R.; McMichael, A.; Fry, D. W. Tyrosine kinase inhibitors. 5. Synthesis and structure–activity relationships for 4-[(phenylmethyl)amino]- and 4-(phenylamino)quinazolines as potent adenosine 5'-triphosphate binding site inhibitors of the tyrosine kinase domain of the epidermal growth factor receptor. *J. Med. Chem.* **1995**, *38*, 3482–3487.
- (42) Rewcastle, G. W.; Palmer, B. D.; Thompson, A. M.; Bridges, A. J.; Cody, D. R.; Zhou, H.; Fry, D. W.; McMichael, A.; Kraker, A. J.; Denny, W. A. Tyrosine kinase inhibitors. 10. Isomeric 4-[(3-bromophenyl)amino]pyrido[d]pyrimidines are potent ATP Binding site inhibitors of the tyrosine kinase function of the epidermal growth factor receptor. *J. Med. Chem.* **1996**, *39*, 1823–1835.

- (43) Olomucki, M.; Marszak, I. The unsaturated amino acids. Synthesis of 4-dimethylamino-2-butynoic acid and 5-dimethylamino-2-pentynoic acid as well as their corresponding esters. *C. R. Hebd. Seances Acad. Sci.* **1956**, *242*, 1338–1340.
- (44) Johnson, C. D.; Lane, S.; Edwards, P. N.; Taylor, P. J. Prodrugs based on masked lactones. Cyclization of γ -hydroxy amides. *J. Org. Chem.* **1988**, *53*, 5130–5139.
- (45) Apodaca, R.; Xiao, W.; Jablonoski, J. A. Preparation of substituted phenylalkynes for use in histamine-mediated disorders. PCT Int. Appl. WO 2003050099 A1, 2003.
- (46) Turner, S. C.; Esbenshade, T. A.; Bennani, Y. L.; Hancock, A. A. A new class of histamine H₃-receptor antagonists: synthesis and structure–activity relationships of 7,8,9,10-tetrahydro-6*H*-cyclohepta-[*b*]quinolines. *Bioorg. Med. Chem. Lett.* **2003**, *13*, 2131–2135.
- (47) Comess, K. M.; Erickson, S. A.; Henkin, J.; Kalvin, D. M.; Kawai, M.; Kim, K. H.; Bamaung, N. Y.; Park, C. H.; Sheppard, G. S.; Vasudevan, A.; Wang, J.; Barnes, D. M.; Fidanze, S. D.; Kolaczowski, L.; Mantei, R. A.; Park, D. C.; Sanders, W. J.; Tedrow, J. S.; Wang, G. T. Preparation of sulfonamides having antiangiogenic and anticancer activity. PCT Int. Appl. WO 2004033419 A1, 2004.
- (48) Chou, T. C.; Talalay, P. Applications of the Median-Effect Principle for the Assessment of Low-Dose Risk of Carcinogens and for the Quantitation of Synergism and Antagonism of Chemotherapeutic Agents. *Bristol-Myers Cancer Symp., New Ave. Dev. Cancer Chemother.* **1987**, *8*, 37–64.
- (49) Cohen, B. D.; Goldstein, D. J.; Rutledge, L.; Vass, W. C.; Lowy, D. R.; Schlegel, R.; Schiller, J. T. Transformation-specific interaction of the bovine papillomavirus E5 oncoprotein with the platelet-derived growth factor receptor transmembrane domain and the epidermal growth factor receptor cytoplasmic domain. *J. Virol.* **1993**, *67*, 5303–5511.
- (50) Fry, D. W.; Nelson, J. M.; Slintak, V.; Keller, P. R.; Rewcastle, G. W.; Denny, W. A.; Zhou, H.; Bridges, A. J. Biochemical and antiproliferative properties of 4-[ar(alk)ylamino]pyridopyrimidines, a new chemical class of potent and specific epidermal growth factor receptor tyrosine kinase inhibitor. *Biochem. Pharmacol.* **1997**, *54*, 877–887.
- (51) Schabel, F. M., Jr.; Griswold, D. P., Jr.; Laster, W. R., Jr.; Corbett, T. H.; Lloyd, H. H. Quantitative evaluation of anticancer agent activity in experimental animals. *Pharmacol. Ther.* **1977**, *1*, 411–435.
- (52) Leopold, W. R.; Nelson, J. M.; Plowman, J.; Jackson, R. C. Anthrapyrazoles, a new class of intercalating agents with high-level, broad spectrum activity against murine tumors. *Cancer Res.* **1985**, *45*, 5532–5539.
- (53) Elliott, W. L.; Howard, C. T.; Dykes, D. J.; Leopold, W. R. Sequence and schedule-dependent synergy of trimetrexate in combination with 5-fluorouracil in vitro and in mice. *Cancer Res.* **1989**, *49*, 5586–5590.
- (54) Elliott, W. L.; Roberts, B. J.; Howard, C. T.; Leopold, W. R. Chemotherapy with [SP-4-3-(*R*)]-[1,1-cyclobutanedicarboxylato (2-)] (2-methyl-1,4-butanediamine-*N,N'*) platinum (CI-973, NK121) in combination with standard agents against murine tumors in vivo. *Cancer Res.* **1994**, *54*, 4412–4418.
- (55) Bridges, A. J.; Denny, W. A.; Dobrusin, E. M.; Doherty, A. M.; Fry, D. W.; McNamara, D. J.; Showalter, H. D. H.; Smaill, J. B.; Zhou, H. Preparation of *N*-quinazolinyllacrylamides and analogues as tyrosine kinase inhibitors. PCT Int. Appl. WO 9738983 A1, 1997; 194 pp.

JM050936O